Conjugative plasmid transfer is limited by prophages but can be overcome by high conjugation rates

Claudia Igler[1*], Lukas Schwyter[1], Daniel Gehrig[1], Carolin Charlotte Wendling[1*]

Affiliation:

[1] ETH Zürich, Institute of Integrative Biology, Universitätstrasse 16, 8092 Zürich, Switzerland

*Corresponding authors: carolin.wendling@env.ethz.ch, claudia.igler@env.ethz.ch

Author contributions: CCW and CI obtained funding, CCW designed the experiments, CI developed the model and run the simulations, LS and DG performed experimental work, CCW analysed experimental data, CCW and CI interpreted the data and wrote the manuscript, all authors commented on the final version of the manuscript.

Acknowledgements: We thank Alex Hall for his valuable input during experimental design and data interpretation, and Thomas Roth for his support during the experimental work. Special thanks go to Hélène Chabas and Roland Regös for their comments on an earlier version of this manuscript. This project has received funding from the Swiss National Science Foundation (grant number PZ00P3_179743) given to CCW and was supported by an ETH Zurich Postdoctoral Fellowship (19-2 FEL-74) received by CI.

Competing interests: The authors have no conflict of interest to declare.

Data accessibility statement: Data have been deposited at dryad; a link will be provided upon acceptance of the manuscript.

Abstract

Antibiotic resistance spread via plasmids is a serious threat to successful treatment and makes understanding plasmid transfer in nature crucial to preventing the global rise of antibiotic resistance. However, plasmid dynamics have so far neglected one omnipresent factor: active prophages (phages that are integrated into the bacterial genome), whose activation can kill co-occurring bacteria. To investigate how prophages influence the spread of a multi-drug resistant plasmid, we combined experiments and mathematical modelling. Using *E. coli*, prophage lambda and the plasmid Rp4 we find that prophages clearly limit the spread of conjugative plasmids. This effect was even more pronounced when we studied this interaction in a 'phage-friendly' environment that favoured phage adsorption. Our empirically parameterized model reproduces experimental dynamics in some environments well, but fails to predict them in others, suggesting more complex interactions between plasmid and prophage infection dynamics. Varying phage and plasmid infection parameters over an empirically realistic range suggests that plasmids can overcome the negative impact of prophages through high conjugation rates. Overall, we find that the presence of prophages introduces an additional death rate for plasmid carriers, the magnitude of which is determined in non-trivial ways by the environment, the phage and the plasmid.

Keywords (3-6):

Horizontal gene transfer, prophages, plasmids, mobile genetic elements, conjugation, co-infection

Introduction

Conjugative plasmids, which can mediate their own horizontal transmission, are important vectors of horizontal gene transfer in prokaryotes and a key source of microbial genetic diversity. Many conjugative plasmids carry accessory genes, which can confer resistance to heavy metals or antibiotics [1, 2]. Understanding plasmid dynamics is therefore not only important to understanding bacterial ecology and evolution in general, but also to predict the rise of antibiotic resistance.

Even though plasmids are widespread among bacterial pathogens in nature, how they spread among bacterial populations is mostly studied in isolated environments. Yet, wherever plasmids and their host bacteria exist, they are generally surrounded by a diverse repertoire of bacteriophages [3]. Thus, it is crucial to understand how plasmids spread in the presence of phages and how such plasmid-phage interactions are shaped by their infection characteristics, for instance their transfer rates, or by environmental conditions.

Overall, bacteriophages are a major cause of bacterial mortality through host cell lysis [4, 5]. These strong reductions in bacterial densities can for instance limit plasmid persistence and spread, and can even drive plasmids to extinction - especially when plasmids do not confer a fitness benefit to their hosts [6]. So far, the impact of phages on plasmid dynamics has only been studied for lytic phages [6], whose infection always leads to host lysis. In contrast, plasmid-phage interactions using temperate phages, which can also integrate their own genetic material into the bacterial chromosome (thereby becoming a prophage), have, to our knowledge, not been studied yet.

Upon infection of a bacterial host cell, temperate phages can choose between a lytic or a lysogenic life cycle. When the ratio of phages to bacterial cells, is low, they mainly go through lytic infections. In contrast, at high phage-to-bacteria ratios, temperate phages preferably form lysogens, i.e., bacteria containing prophages [7, 8]. However, prophages can switch to the lytic cycle to replicate, assemble progeny and ultimately kill their hosts through lysis [9]. This switch happens either spontaneously (at low rates) or in response to stressful conditions (at high rates). Released phages can then kill

73 competing cells that are susceptible to these phages because they are not carrying the respective
74 prophage, which usually confers protection against superinfection [10, 11].

75 Considering that prophages are found in more than 50% of bacterial genomes, in which they can
76 constitute up to 10-20% of the genome [12], prophages are likely to influence plasmid dynamics -
77 which can occur in various ways and is not necessarily as obvious as for lytic phages [6] given the
78 complexity of their lifestyle. Released phages can for instance kill plasmid donor or recipient cells,
79 which will negatively influence plasmid spread and persistence. On the other hand, resident
80 prophages will also protect plasmids carried in the same host cell from lytic infections of related
81 phages due to superinfection immunity. Given the dynamic nature of phage and plasmid infections,
82 the outcome might be very specific to a given prophage-plasmid pair, but potentially there are more
83 general interaction patterns to be discovered.

84 Here, we experimentally investigated how the presence of a prophage and environmental
85 conditions influence plasmid dynamics in *E. coli*, using its naturally associated prophage lambda
86 together with the conjugative multidrug-resistant plasmid Rp4. A mathematical model allowed us to
87 explain the observed dynamics and to test the generality of our results by varying phage and plasmid
88 infection parameters over a wide range that captures empirically reported values. Model predictions
89 of plasmid spread in a new environment agree with experimental observations qualitatively but not
90 quantitatively, indicating unknown interactions that deserve further exploration. Overall, we find that
91 prophages can limit plasmid spread substantially by effectively introducing an additional death rate.
92 Consequently, our model predicts for example the evolution of higher plasmid conjugation rates in
93 phage-rich environments in order to overcome this additional death rate.

94 # Material and Methods

95 ## Experimental work

96 Strains, media and culture conditions

97 All experiments were carried out in liquid LB ('LB') or liquid LB supplemented with 10% SM
98 Buffer (9.9 mM NaCl, 0.8 mM MgSO4 × 7 H_2O, and 5 mM Tris-HCl) ('SM'). Antibiotics were used
99 at the following concentrations, unless otherwise noted: Ampicillin (amp): 100 μg ml^{-1}; kanamycin
100 (kan): 50 μg ml^{-1}, tetracycline (tet) and chloramphenicol (cm): 25 μg ml^{-1}. Mitomycin C was used at
101 a concentration of 0.5 μg ml^{-1}.

102 All bacterial strains used in the present study were designed from wildtype *E. coli* K-12 MG1655
103 (WT; Table 1). We used three different donor strains: (1) a plasmid donor, which carried the Rp4
104 plasmid conferring resistance to three different antibiotics: ampicillin (amp^R), kanamycin (kan^R), and
105 tetracyclin (tet^R), (2) a phage donor, i.e., a lysogen carrying the prophage lambda which encoded an
106 ampicillin resistance gene, and (3) a plasmid-phage-donor, which carried both, the Rp4 plasmid and
107 the lambda prophage. Lysogen construction was done as described in [10]. In addition, the phage
108 donor and the plasmid-phage-donor, were both labelled with a yellow-super-fluorescent protein
109 (SYFP) marker [13]. The recipient was labelled with a dTomato fluorescent protein and carried a
110 chloramphenicol (cm^R) resistance gene. Strains were grown in LB-medium (Lysogeny Broth, Sigma-
111 Aldrich) at 37° C with constant shaking at 180 rpm.

112 **Table 1** Strains and phage used in the present study

Strain/ Phage	Characteristics
Wild type	*E. coli* K-12 MG1655
Plasmid donor	Rp4 plasmid (amp^R, kan^R, tet^R)
Phage donor	YFP, lambda+ bor::amp^R
Plasmid-phage-donor	YFP, lambda+ bor::amp^R, Rp4 plasmid (amp^R, kan^R, tet^R)
Recipient	dTomato cm^R
Lambda+	Δ(bor)::amp

113

114 Bacterial and phage densities

115 Total bacterial counts were determined by plating out 25 μl of a dilution series ranging from 10^{-1}
116 to 10^{-6} on LB-agar plates (Sigma-Aldrich). To identify recipient strains (carrying the RFP marker) we
117 took pictures of each plate using a ChemiDoc XRS+ and subsequently counted the colonies using
118 ImageJ with the PlugIn CellCounter for manual cell count. To determine phage donors (carrying the
119 YFP marker) we used a blue light. Further discriminations between all possible strains and prophage-
120 plasmid combinations were achieved by replica plating (details are described below for each
121 experiment separately). All plates were incubated overnight at 37°C and the total amount of colonies
122 was counted the following day. The amount of free viral particles (PFU/ml) per culture was
123 determined using a standard spot assay, where 2 μl of a dilution series of phages ranging from 10^{-1} to
124 10^{-8} diluted in SM-Buffer was spotted onto 100 μl indicator cells of the WT grown in 3 ml of 0.7%
125 soft-agar. To obtain indicator cells we centrifuged 15 ml of an exponentially growing WT culture for
126 10 min at 5000 rpm, resuspended the pellet in 2 ml 10mM MgSO4 and incubated the mixture for
127 another hour at 37° C with constant shaking.

128

129 Experimental design

130 We used two different mono-culture experiments to determine conjugation- and overall
131 lysogenization- (meaning lysogen appearance, which subsumes various processed like induction,
132 adsorption and life-cycle decision making) rates in LB and SM respectively. This was followed by
133 an experiment in which we co-cultured the recipient with both donor strains (referred to as two-donor
134 experiment), one harbouring the plasmid and one the prophage, to investigate how the presence of
135 prophages influences plasmid dynamics and how this depends on the environment (LB or SM). To
136 test model predictions, we performed a third experiment in which we cocultured the recipient with
137 the phage-plasmid-donor that harboured the plasmid and the prophage simultaneously (referred to as
138 one-donor experiment). In this experiment, we additionally looked at how different starting cell-
139 densities influence plasmid dynamics in the presence of LB and SM. Each experiment was done with

140 three to four (mono-culture experiment) or six (one- and two-donor experiments) independent
141 biological replicates. For each replicate, single colonies of each strain were inoculated in 6 ml of LB
142 and grown overnight. The following day we determined the optical density of each overnight culture
143 at 600 nm using an automated plate-reader (Tecan infinite 200) and adjusted the OD of each culture
144 to the lowest measured OD, to obtain similar starting concentrations of each subpopulation per
145 culture.
146
147 Mono-culture experiments: To determine the conjugation rate of Rp4 or the 'lysogenization' rate
148 of phage lambda, we diluted the OD-adjusted overnight cultures of donors (either the phage or the
149 plasmid donor) and recipients 1:30 in each of the two environments and subsequently added 300 μl
150 of each dilution to 5400 μl LB or LB+SM, respectively. This resulted in a starting concentration of
151 approximately 2×10^6 CFU/ml of each strain. We then determined PFU/ml and CFU/ml from seven
152 time-points, i.e., T0 immediately after mixing, T1-T7 corresponding to 1, 2, 3, 5, and 7 hpm (hours
153 post mixing) and T24 at 24 hpm. CFU/ml was determined by selective plating on LB to estimate the
154 total population density and LB supplemented with cm and amp to select for transconjugants
155 (recipient plasmid carriers) or on LB supplemented with amp to select for new lysogens (recipient
156 carrying the prophage). As we had to adjust the dilutions that we chose to plate out to obtain the total
157 population density, this introduced a detection limit of approximately 10^3 CFU/ml for individual
158 subpopulations.
159
160 Two-donor experiments: To determine how prophages influence plasmid dynamics we co-cultured
161 both donor strains and the recipient strain at equal starting concentrations of approximately 3×10^7
162 of each strain type. OD-adjustment and dilutions were done as described above for the two-species
163 experiments. Plating at selected time points (T0 – T24, as described for the mono-culture experiment)
164 was done on (1) LB-agar to obtain total community densities, (2) LB-agar + kan to select for all
165 plasmid-carrying strains, (3) LB-agar + cm to select for all recipients. Subsequently LB-agar + cm

166 plates were stamped on three different selective agar plates: (3.1) LB as a reference for total cell
167 count, (3.2) LB-agar + amp to select for recipient strains that have acquired the phage, the plasmid or
168 both, (3.3) LB-agar + kan to select for recipient strains that have acquired the plasmid. Colonies from
169 plates (1) and (2) were further discriminated based on the fluorescent marker (YFP marker: phage or
170 plasmid donor, dTomato: recipient). In addition, we screened a subset of amp resistant recipients
171 (n=24) for phage presence using a mitomycin C induction followed by a spot-assay on the WT to
172 estimate the proportion of lysogens and transconjugants, which are both resistant to ampicillin.
173 To determine whether resistance against the ancestral phage had emerged we picked 40 colonies
174 each, from recipients and plasmid donors from each replicate after 24 hours. From each colony we
175 generated indicator cells to be used in a standard spot assay in which we spotted 2 μl of the ancestral
176 phage on a 3 ml lawn containing 100 μl indicator cells. No plaque formation indicated resistance
177 evolution.
178
179 <u>One-donor experiment</u>: To validate our model predictions, that a single donor, carrying the phage
180 and the plasmid in combination with high starting population densities will favour conjugation, we
181 performed a separate experiment using four different environments, i.e., LB/high, LB/low, SM/high,
182 SM/low, where high and low correspond to the total population density at the onset of the experiment
183 (high: ~8.75 ± 0.02 CFU/ml (s.e.); low: ~6.53 ± 0.03 CFU/ml (s.e.)). As plasmid donors were heavily
184 lysed during the two-donor experiment we now used a plasmid-phage-donor, that carried both, the
185 prophage and the plasmid, giving the plasmids an additional advantage through prophage-conferred
186 immunity to further phage infections. OD-adjustments and dilutions were done as described above
187 and the total populations were plated on selective plates at four selected timepoints, i.e., T0, T2, T5,
188 and T24 hpm. We discriminated the different colony types by selective and replica plating on LB-
189 agar plates carrying different antibiotics and based on their fluorescent marker as described for the
190 two-donor experiment. As above, we screened a subset of colonies (n=24) for phage presence using
191 mitomycin C induction followed by a spot-assays on the WT.

192

193 Estimating fitness cost of plasmid carriage: To better parameterize our model, we determined
194 fitness costs associated with plasmid carriage using pairwise competition assays as described in [10].
195 Briefly, overnight cultures of competing strains were cocultured in LB at a ratio of 1:1 and grown for
196 24 hours. Total cell densities were determined at 0 and 24 hours post mixing by selective plating.
197 Relative fitness (W) of strain A to strain B was calculated using the ratio of Malthusian parameters
198 of both competing strains [14], according to the following formula:

199

200 $$W=\frac{ln(abundance_{t=24})/abundance_{t=0})_{strainA}}{ln(abundance_{t=24})/abundance_{t=0})_{strainB}}$$

201

202 There were no significant fitness costs for recipients for carrying the fluorescent and the
203 chloramphenicol marker (Figure S5), nor when recipients acquired the plasmid (Figure S5) or the
204 prophage [10].

205

206 Statistical analysis

207 *Transfer rates*: To determine plasmid and phage transfer rates (overall lysogenization and conjugation
208 rate), we estimated the proportion of the curve that is linear during exponential increase of
209 transconjugants and new lysogens and fitted a linear regression to the data with log10 transformed
210 colony forming units as dependent variable and time as fixed effect. We then used the slope of the
211 regression line as a proxy for plasmid or phage transfer over time during exponential growth. To
212 determine differences in transfer rates between plasmids and phages or environments (LB or SM) we
213 performed a Welch's two sample *t*-test. Note, this method did not directly quantify conjugation and
214 lysogenization rate *per se*, but rather gives a proxy for the spread of the plasmid or the phage based
215 on these different recipient populations due to vertical and horizontal transmission.

216

217 *Absolute numbers*: To determine differences between the total amount of transconjugants and
218 lysogens after 24 hours in LB and SM, we performed Welch's two sample *t*-tests for each
219 environment. Differences in the amount of lysogens as well as transconjugants over time between
220 both environments were analysed using a generalized least squares model to control for
221 autocorrelation of residuals over time using the gls function (package nlme) with medium (LB/SM),
222 and time as well as their interaction as fixed effect.
223
224 **Mathematical model of phage and plasmid transfer dynamics**
225 We used a mathematical model to describe the dynamics of various bacterial populations (empty
226 recipients, plasmid carriers and lysogens) as well as the phage population, making the following
227 assumptions: As all species are generally found at high numbers, we used a deterministic model.
228 Further, because phage and plasmid infection dynamics show a significant, but 'fixed' time delay
229 (due to, either the time spent within the cell for reproduction, or the time necessary for DNA transfer),
230 we used delay-differential equations (dde23 solver; Matlab R2019a (The MathWorks, Natick, MA,
231 USA)). Lastly, as experimental cultures were grown in liquid medium with shaking, we assumed a
232 well-mixed environment, where plasmid transfer and phage infections can be described via mass
233 action kinetics. Population dynamic simulations were run for 24h, using starting densities and most
234 parameters fitted to empirical data (Table S1).
235
236 <u>Two-donor model (Figure 1E, equations 1-18)</u>
237 Bacterial cells grow at a net growth rate r (summarizing growth and death) until they reach
238 carrying capacity K. Cells carrying the plasmid or the prophage grow at r_p and r_l respectively,
239 assuming a (minor) growth cost. The plasmid can be transferred from the plasmid donor (DP) to
240 recipient cells (R), phage donors (DL) or recipient lysogens (RL) with a certain conjugation rate (p),
241 leading to recipient plasmid (RP), recipient lysogen plasmid (RLP) and phage donor plasmid (DLP)
242 cells after τ_p time units needed for transfer. Plasmids can be transferred from any plasmid-carrying

243 population, but conjugation slows down when cells approach stationary phase [15, 16] - which is
244 scaled via k_p (Equ. 16), as our empirical data suggested that conjugation is not completely inhibited
245 during stationary phase (see increase of transconjugants and double-carriers from T7 to T24 in Figure
246 1B). Including segregation loss of plasmids did not improve our model fit with experimental data.

247 Similarly, phages can infect recipient cells, plasmid donors (*DP*) and recipient plasmid carriers
248 (*RP*), which results in a decision (after τ_d time units) for lysogeny with a probability *l* (*RL*, *DPL* and
249 *RPL* respectively), or for lysis at a rate (1-*l*) producing β new virions after τ_l time units. As has been
250 shown before [17, 18], the lysogenization probability is dependent on the number of phages infecting
251 a bacterial host cell and is hence a function of the number of free phages, which has been modelled
252 via a power-law exponent (Equ. 14). Assuming that phage induction only occurs through spontaneous
253 induction, prophages are induced at a low constant rate *i* to produce new virions (in addition to lysis
254 at infection) after τ_i time units.

255 Phages are lost by attaching to lysogen cells, which cannot be productively infected due to
256 superinfection immunity of the prophage residing within the lysogen. The adsorption rate α is
257 dependent on the physiological state of the host bacteria and saturates with *K* [19, 20] – we found that
258 the best fit to our data came from a steep response to the approach of stationary phase, which we
259 included via a power-law exponent, but a weaker final reduction, as scaled by k_a (Equ.15). The
260 efficiency of adsorption effectively decreases if several phages are infecting one cell, because one
261 phage would be already sufficient for infection. Hence, we modify the absorption rate also by the
262 number of virions via a saturating Hill function [21] (Equ.15). Further, we included additional (sub-
263)populations with lower adsorption rates, as we saw that recipient and donor plasmid cells regrew
264 after an initial drop in cell numbers but did not find genetically resistant cells at the end of the
265 experiment. This phenomenon is called phenotypic resistance [22], meaning that the population
266 shows heterogeneity in adsorption rates (e.g., by expressing different amounts of the lambda
267 receptor). Specifically, this was modeled using recipient, plasmid donor and recipient plasmid
268 subpopulations (*RR*, *RPR* and *DPR*) with lower phage adsorption rates (α_2). For simplicity we only

modeled switching into the state of 'phenotypic resistance' at rate μ, but including a back-switching rate did not significantly change our results.

Note that for simplicity, we model plasmid and phage transfer to the same host as a sequential process but including the possibility of transfer of both plasmid and phage to recipients at the same time did not change our results notably due to the low probability of these events.

The processes described above are summarized in the following equations (with purple denoting bacterial growth, red switching into phenotypic resistance, blue phage infection and lysogenization, brown phage induction and replication via cell burst, green plasmid conjugation and orange phage death):

$$\frac{dDL}{dt} = r_L \cdot DL \cdot \left(1 - \frac{T}{K}\right) - i \cdot DL(t - \tau_i) - p \cdot DL \cdot P \tag{1}$$

$$\frac{dDP}{dt} = r_P \cdot DP \cdot \left(1 - \frac{T}{K}\right) - \alpha \cdot DP \cdot V - \mu \cdot DP \cdot r_P \cdot \left(1 - \frac{T}{K}\right) \tag{2}$$

$$\frac{dR}{dt} = r \cdot R \cdot \left(1 - \frac{T}{K}\right) - \alpha \cdot R \cdot V - p \cdot R \cdot P - \mu \cdot R \cdot r \cdot \left(1 - \frac{T}{K}\right) \tag{3}$$

$$\frac{dRL}{dt} = r_L \cdot RL \cdot \left(1 - \frac{T}{K}\right) - i \cdot RL(t - \tau_i) + \alpha \cdot l \cdot R(t - \tau_d) \cdot V(t - \tau_d) + \alpha_2 \cdot l \cdot RR(t - \tau_d) \cdot V(t - \tau_d) - p \cdot RL \cdot P \tag{4}$$

$$\frac{dRP}{dt} = r_P \cdot RP \cdot \left(1 - \frac{T}{K}\right) + p \cdot R(t - \tau_p) \cdot P(t - \tau_p) - \alpha \cdot RP \cdot V - \mu \cdot RP \cdot r \cdot \left(1 - \frac{T}{K}\right) \tag{5}$$

$$\frac{dDLP}{dt} = r_P \cdot DLP \cdot \left(1 - \frac{T}{K}\right) + p \cdot DL(t - \tau_p) \cdot P(t - \tau_p) - i \cdot DLP(t - \tau_i) \tag{6}$$

$$\frac{dDPL}{dt} = r_L \cdot DPL \cdot \left(1 - \frac{T}{K}\right) + \alpha \cdot l \cdot DP(t - \tau_d) \cdot V(t - \tau_d) + \alpha_2 \cdot l \cdot DPR(t - \tau_d) \cdot V(t - \tau_d) - i \cdot DPL(t - \tau$$

$$\frac{dRLP}{dt} = r_L \cdot RLP \cdot \left(1 - \frac{T}{K}\right) + p \cdot RL(t - \tau_p) \cdot P(t - \tau_p) - i \cdot RLP(t - \tau_i) \tag{8}$$

$$\frac{dRPL}{dt} = r_L \cdot RPL \cdot \left(1 - \frac{T}{K}\right) + \alpha \cdot l \cdot RP(t - \tau_d) \cdot V(t - \tau_d) + \alpha_2 \cdot l \cdot RPR(t - \tau_d) \cdot V(t - \tau_d) - i \cdot RPL(t - \tau$$

$$\frac{dRR}{dt} = r \cdot RR \cdot \left(1 - \frac{T}{K}\right) + \mu \cdot R \cdot r \cdot \left(1 - \frac{T}{K}\right) - \alpha_2 \cdot RR \cdot V - p \cdot RR \cdot P \tag{10}$$

$$\frac{dRPR}{dt} = r_P \cdot RPR \cdot \left(1 - \frac{T}{K}\right) + \mu \cdot RP \cdot r \cdot \left(1 - \frac{T}{K}\right) - \alpha_2 \cdot RPR \cdot V + p \cdot RR(t - \tau_p) \cdot P(t - \tau_p) \tag{11}$$

$$\frac{dDPR}{dt} = r_P \cdot DPR \cdot \left(1 - \frac{T}{K}\right) + \mu \cdot DP \cdot r \cdot \left(1 - \frac{T}{K}\right) - \alpha_2 \cdot DPR \cdot V \tag{12}$$

$$\frac{dV}{dt} = i \cdot \beta \cdot (DL(t-\tau_i) + RL(t-\tau_i) + RLP(t-\tau_i) + RPL(t-\tau_i) + DLP(t-\tau_i) + DPL(t-\tau_i)) - \gamma_V \cdot V + \alpha \cdot (1-l) \cdot \beta \cdot V(t-\tau_l) \cdot (R(t-\tau_l) + RP(t-\tau_l) + DP(t-\tau_l)) - \alpha \cdot V \cdot (R + RL + DL + RP + DP + RLP + RPL + DLP + DPL) + \alpha_2 \cdot (1-l) \cdot \beta \cdot V(t-\tau_l) \cdot (RR(t-\tau_l) + RPR(t-\tau_l) + DPR(t-\tau_l)) - \alpha_2 \cdot V \cdot (RR + RPR + DPR) \quad (13)$$

$$with \ l = l_1 \cdot V^{l_2} \quad (14)$$

$$\alpha = \alpha' \cdot \frac{1}{1 + \frac{V}{V_c}} \cdot \left(1 - k_a \cdot \frac{T}{K}\right)^{k_2} \quad (15)$$

$$p = p' \cdot \left(1 - k_p \cdot \frac{T}{K}\right) \quad (16)$$

$$T = DL + DP + R + RL + RP + DLP + DPL + RPL + RLP + RR + RPR + DPR \quad (17)$$

$$P = DP + RP + RPL + RLP + DPL + DLP + RPR + DPR \quad (18)$$

Parameter estimation from the experiments

Plasmid and overall phage transfer rate parameters were inferred from mono-culture experiments by fitting to the ratio of transconjugants or lysogens over the whole population (transconjugants or lysogens plus recipient cells): *T/(T+R)* [23]. This generally only holds true for initial dynamics where horizontal gene transfer outweighs vertical transmission, but conjugation rates were not vastly different for early (between T4 and T6) and late dynamics (T12 and T24) in our experiments. The duration of plasmid transfer was estimated from the initial lag time and the steepness of the increase. For phage infection parameters (i.e., adsorption, induction and lysogenization rate) we started out with literature values and refined the fit to the observed overall phage transfer rate. Further, phage burst size and latent period (time delay from adsorption to burst) were determined from one-step growth curves as the time until phage numbers start to rise (minimal latent period) and the final number of phages when phage increase levels off, relative to the starting phage number. Bacterial growth rates of donor, recipient (r), transconjugant (r_p), and lysogen (r_l) cells were fitted via linear

329 regression to the slope of growth measurements for the individual populations (giving an effective
330 growth rate, which includes cell growth and death).
331
332 Analysis of the sensitivity of model predictions to parameter variation
333 We performed parameter sensitivity analyses for the two-donor experiments (Figure 2, S1-S3)
334 by varying adsorption rate [24, 25], conjugation rate [26], lysogenization probability [27], induction
335 rate [27-30], growth rate, and starting bacterial density over a wide range of parameters including
336 empirically observed values. In simulations where adsorption rate was kept constant, we used the
337 lower adsorption rate of LB environments. Contour plots show the absolute cell numbers of various
338 subpopulations at the end of a 24h-simulation run.
339
340 One-donor model (Figure S4, equations 19-31)
341 The one-donor model is a simplified version of the two-donor model, starting from a recipient
342 (*R*) and a single donor, which contains the plasmid and the prophage (*D*). This donor can transfer
343 phages and plasmids (while also being lysed according to the phage induction rate), yielding recipient
344 lysogens (*RL*), recipient plasmid (*RP*) and subsequently recipient lysogen plasmid carriers (*RPL*). We
345 again include phenotypically resistant subpopulations of lower adsorption rate (*RR*, *RPR*) and use the
346 same parameter dependencies on bacteria and/or phage numbers as described above.
347 These processes are summarized in the following equations (with purple denoting bacterial
348 growth, red switching into phenotypic resistance, blue phage infection and lysogenization, brown
349 phage induction and replication via cell burst, green plasmid conjugation and orange phage death):
350

$$\frac{dD}{dt} = r \cdot D \cdot \left(1 - \frac{T}{K}\right) - i \cdot D(t - \tau_i) \tag{19}$$

$$\frac{dR}{dt} = r \cdot R \cdot \left(1 - \frac{T}{K}\right) - \alpha \cdot R \cdot V - p \cdot R \cdot P - \mu \cdot R \cdot r \cdot \left(1 - \frac{T}{K}\right) \tag{20}$$

$$\frac{dRL}{dt} = r_L \cdot RL \cdot \left(1 - \frac{T}{K}\right) - i \cdot RL(t - \tau_i) + \alpha \cdot l \cdot R(t - \tau_d) \cdot V(t - \tau_d) + \alpha_2 \cdot l \cdot RR(t - \tau_d) \cdot V(t - \tau_d) - p \cdot RL \cdot P \tag{21}$$

$$\frac{dRP}{dt} = r_P \cdot RP \cdot \left(1 - \frac{T}{K}\right) + p \cdot R(t - \tau_p) \cdot P(t - \tau_p) - \alpha \cdot RP \cdot V - \mu \cdot RP \cdot r \cdot \left(1 - \frac{T}{K}\right) \tag{22}$$

$$\frac{dRPL}{dt} = r_L \cdot RPL \cdot \left(1 - \frac{T}{K}\right) + p \cdot RL(t - \tau_p) \cdot P(t - \tau_p) + \alpha \cdot l \cdot RP(t - \tau_d) \cdot V(t - \tau_d) + \alpha_2 \cdot l \cdot RPR(t - \tau_d) \cdot V(t - \tau_d) - i \cdot RPL(t - \tau_i) \tag{23}$$

$$\frac{dRR}{dt} = r \cdot RR \cdot \left(1 - \frac{T}{K}\right) + \mu \cdot R \cdot r \cdot \left(1 - \frac{T}{K}\right) - \alpha_2 \cdot RR \cdot V - p \cdot RR \cdot P \tag{24}$$

$$\frac{dRPR}{dt} = r_P \cdot RPR \cdot \left(1 - \frac{T}{K}\right) + \mu \cdot RP \cdot r \cdot \left(1 - \frac{T}{K}\right) - \alpha_2 \cdot RPR \cdot V + p \cdot RR(t - \tau_p) \cdot P(t - \tau_p) \tag{25}$$

$$\frac{dV}{dt} = i \cdot \beta \cdot (D(t - \tau_i) + RL(t - \tau_i) + RPL(t - \tau_i)) - \gamma_V \cdot V + \alpha \cdot (1 - l) \cdot \beta \cdot V(t - \tau_l) \cdot (R(t - \tau_l) + RP(t - \tau_l)) - \alpha \cdot V \cdot (D + R + RL + RP + RPL) + \alpha_2 \cdot (1 - l) \cdot \beta \cdot V(t - \tau_l) \cdot (RR(t - \tau_l) + RPR(t - \tau_l)) - \alpha_2 \cdot V \cdot (RR + RPR) \tag{26}$$

$$with\ l = l_1 \cdot V^{l_2} \tag{27}$$

$$\alpha = \alpha' \cdot \frac{1}{1 + \frac{V}{V_c}} \cdot \left(1 - k_a \cdot \frac{T}{K}\right)^{k_2} \tag{28}$$

$$p = p' \cdot \left(1 - k_p \cdot \frac{T}{K}\right) \tag{29}$$

$$T = D + R + RL + RP + RPL + RR + RPR \tag{30}$$

$$P = D + RP + RPL + RPR \tag{31}$$

376 **Results**

377 To determine plasmid dynamics in the presence of a prophage-carrying population, we
378 combined experiments of plasmid spread in the absence (mono-culture experiment) or in the presence
379 of a prophage (two-donor and one-donor experiment) with mathematical modelling. Experiments
380 were performed in a 'standard' liquid environment (rich medium, 'LB') or in a 'phage-friendly'
381 environment (LB supplemented with SM-buffer, 'SM'), which is characterized by increased phage
382 adsorption rates [31].

383

384 *Plasmid spread occurs later than prophage spread, but continues longer than phage infection*

385 First, we determined phage (lysogenization) and plasmid (conjugation) transfer dynamics
386 independently of each other (Figure 1A). Note that free phages were not added externally but resulted
387 from prophage induction and ensuing lytic phage infection. In LB, lysogens appeared considerably
388 earlier than transconjugants (Figure 1B). Even though lysogen formation, i.e., mean number of newly
389 formed lysogens per minute during the exponential increase in lysogens (mean = 0.15 ± 0.009 s.e.),
390 was faster than the formation of transconjugants (mean = 0.13 ± 0.007 s.e.; Figure 1), it also saturated
391 earlier. This resulted in a significantly higher number of transconjugants than lysogens after 24 hours
392 (Welch's two sample *t*-test at T24 in LB: $t_{4.8}$=6.41, p=0.002; Figure 1B).

393 In SM, the initial dynamics were similar to LB (i.e., earlier appearance of lysogens than
394 transconjugants), however, the rate of lysogen formation (mean in SM = 0.203 ± 0.003 s.e.; Welch's
395 two sample *t*-test: $t_{2.65}$=-5.22, p=0.019; Figure 1B) as well as the absolute numbers of lysogens over
396 time (significant time × environment interaction in generalized least squares model $F_{6,27}$=23.82,
397 p<0.001), were significantly higher compared to LB - which explains the approximately equal
398 numbers of transconjugants and lysogens in SM after 24 hours (Welch's two sample *t*-test at T24 in
399 SM: $t_{3.0}$=2.72, p=0.07). This confirms that the high concentration of Mg^{2+} and Cl^{-} ions in the SM
400 environment favoured phage adsorption to recipient cells [31], which resulted in a higher amount of

401 lysogens in SM compared to LB (Figure 1B). Notably, conjugation was not influenced by SM (non-

402 significant time × environment interaction in generalized least squares model $F_{7,47}$=0.98, p=0.45).

403

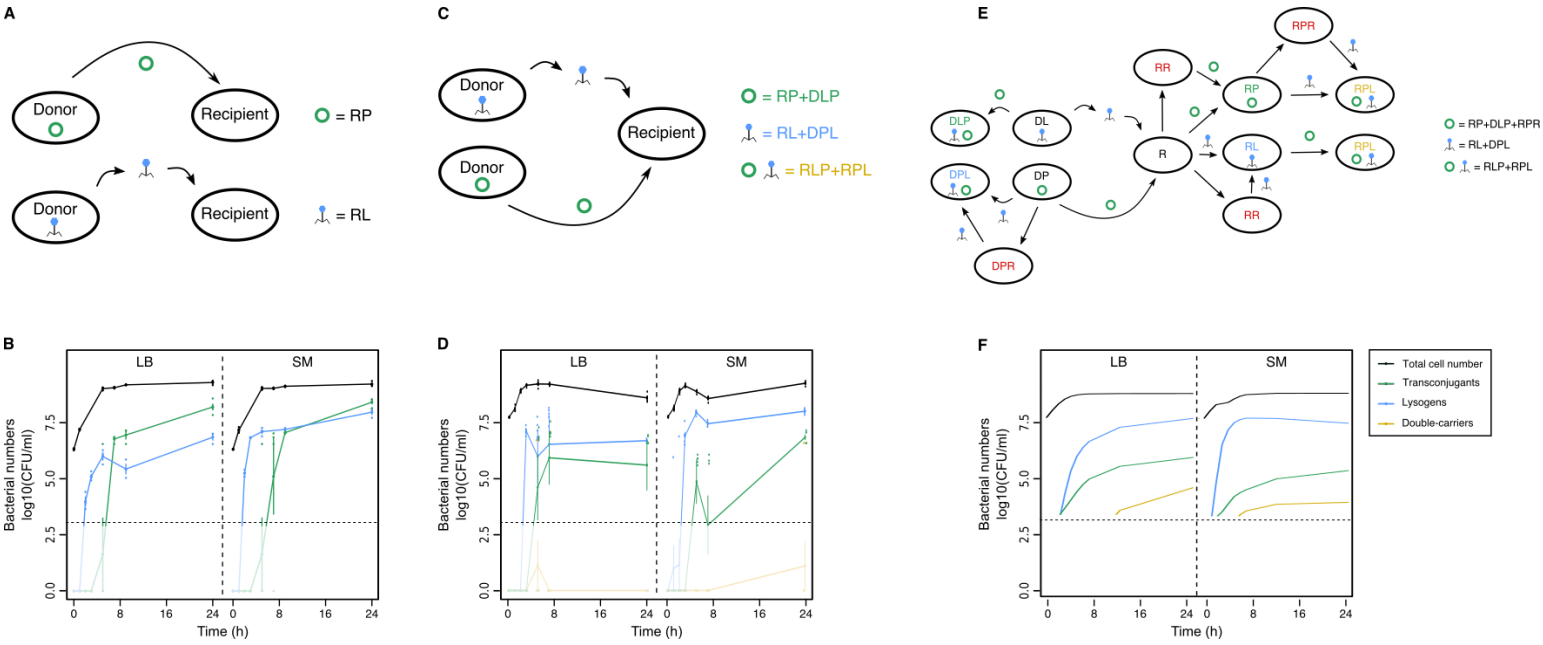

405 **Figure 1 Phage and plasmid transfer with separate donors.** (A) Mono-culture experiments with independent phage and plasmid
406 transfer. (B) Total amount of bacteria (black) newly formed lysogens (blue) and transconjugants (green) measured as colony forming
407 units log10(CFU/ml) over time in LB (left panel) or SM (right panel) in mono-culture experiments. The grey line indicates the detection
408 limit. (C) Two-donor experiments with one donor carrying the plasmid and one carrying the phage. Transconjugants are counted as
409 recipient and lysogen donors, which acquired the plasmid (green), and lysogens as recipients and plasmid donors, which acquired the
410 phage (blue). Double carriers are recipients, that acquired the plasmid and the phage (yellow). (D) Total population size (black) as well
411 as newly formed lysogens (blue), transconjugants (green), and double-carriers (yellow) measured as colony forming units
412 log10(CFU/ml) over time in LB or SM in two-donor experiments. (E) Model reactions and (F) 24h-simulations of phage and plasmid
413 transfer for the two-donor experiment (colours as described in D).

414

415 *Phage infections limit plasmid spread in environments with two donors*

416 Next, we determined the formation of plasmid- and prophage-carrying cells in co-culture with

417 two different donors, one plasmid-donor and one phage-donor, and one recipient (Figure 1C). We

418 observed a faster formation of lysogens (i.e., recipients and plasmid donors that acquired the

419 prophage) than of transconjugants (i.e., recipients and phage donors that acquired the plasmid) at the

420 beginning of the experiment, which agrees with the mono-culture experiments. However, within the

421 given time-frame of 24 hours, the total amount of transconjugants did not exceed the amount of

422 lysogens. In comparison to the mono-culture experiment, we observed a lower initial formation of

423 transconjugants over time, which was significant in SM but not in LB (Welch's two sample *t*-test LB:

424 $t_{3.69}$=-0.99, p=0.38, Welch's two sample *t*-test SM: $t_{3.05}$=5.15, p=0.013). In addition, also the final

425 amount of transconjugants was 1.8 and 1.5 orders of magnitude lower in LB and SM after 24 hours.
426 This indicates a strong negative impact of the released temperate phages on plasmid transfer. In
427 contrast, phage transfer was not negatively affected by plasmids and we even observed a significantly
428 higher formation rate of lysogens in LB and SM (Welch's two sample *t*-test LB: $t_{2.51}$=-13.09, p=0.002,
429 Welch's two sample *t*-test SM: $t_{5.7}$=-8.64, p<0.001) as well as a higher absolute number of lysogens
430 in LB compared to the mono-culture experiment. However, in the initial mono-culture experiment,
431 the starting ratio between donors and recipients was 1:1, whereas in the coculture experiment phage-
432 susceptible bacteria (recipients and plasmid-donors) outnumbered phage-donors 2:1, providing
433 phages with the possibility of higher amplification and likely driving the higher amount of lysogens
434 in the co-culture experiment in LB.
435
436 *A mathematical model qualitatively reproduces empirical data*
437 While it seems intuitive that the presence of phages would limit or slow down plasmid spread
438 through bacterial killing, the low abundance of double-carriers throughout the experiments was
439 surprising, given the abundance of transconjugants and newly formed lysogens after 5hpm. Hence,
440 we used a mathematical model to explore this puzzle in more depth, taking advantage of the parameter
441 values available from our empirical data as well as from the literature (Methods, Table S1). After
442 fitting constant phage and plasmid transfer parameters (adsorption and conjugation, respectively), we
443 found however, that it was necessary to make both rates dependent on bacterial growth (i.e., the
444 carrying capacity) in order to obtain a good qualitative fit to empirically observed dynamics. This is
445 supported by studies showing a decrease of plasmid and phage transfer in stationary phase bacteria
446 [21, 32]. Further, the efficiency of phage adsorption decreases with increasing phage numbers, as
447 more phages adsorb to one bacterial cell, but still produce only one lysogen or one phage burst.
448 Lysogenization rate on the other hand was found to increase with phage density ([17, 18]).
449 Thus, even in this deceptively simple system, consisting of only three players - phages, plasmids
450 and bacterial hosts - the dynamics of the interactions are complex. Still, the model qualitatively

451 reproduced the observed trajectories of lysogens, transconjugants and double-carriers (Figure 1F) as
452 well as the individual subpopulations (Figure S6). The rise of plasmid-carriers occurred earlier in the
453 model, likely because during the initial lag phase conjugation is not well described by mass action
454 kinetics [15] and we overestimated the appearance of transconjugants in this early stage. Notably,
455 while the model also predicted low numbers of double-carriers in LB, they were still higher than
456 observed empirically. To some extent, the fit between model and data is obscured by the detection
457 limit of subpopulations at low numbers, but this discrepancy could also indicate that the model is not
458 capturing all mechanisms relevant to phage or plasmid transfer in our system.
459
460 *The number of transconjugants is dependent on the conjugation rate, but largely independent of*
461 *phage infection parameters*
462 After confirming the fit with our experiments, we used the model to extend our analysis to
463 different plasmid and phage combinations. Therefore, we varied phage and plasmid infection
464 parameters over a wide range that captures previously observed empirical values (Methods). Our
465 main focus was on phage adsorption and plasmid conjugation rate, which can be seen as the most
466 comparable fitness parameter for phage and plasmid transfer [33]. In addition, we also explored
467 changes in other relevant infection parameters, notably lysogenization probability and induction rate,
468 as well as bacterial growth rate and starting population density. (Variations in burst size showed very
469 similar results to variations in induction rate and are not shown.)
470

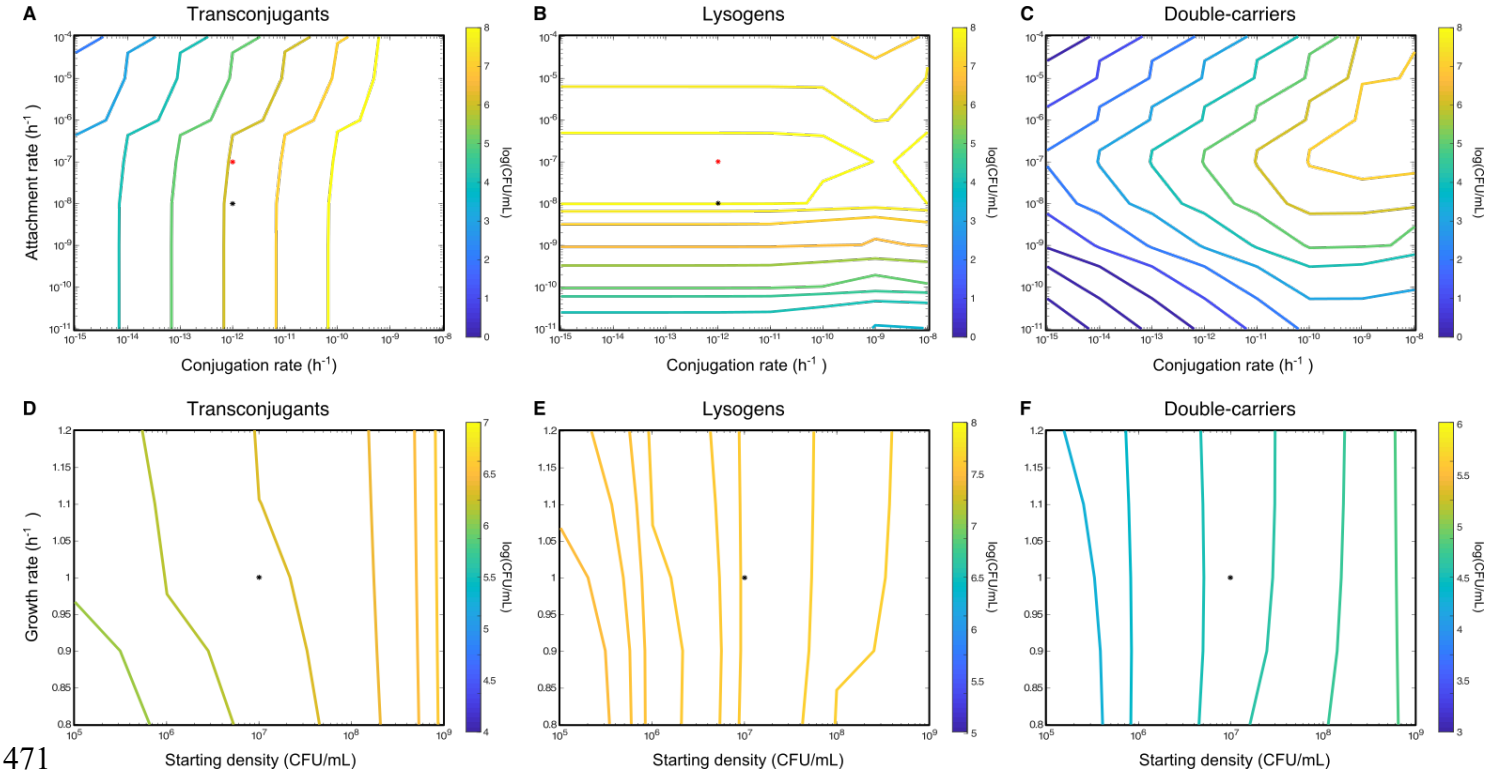

Figure 2 Variation in modelling parameters. Contour plots give the (log-transformed) cell numbers of transconjugants (A, D), new lysogens (B, E) and double-carriers (C, F) in response to variation in adsorption and conjugation rate (top row) or growth rate and starting inoculum size (bottom row) at the end of 24h-simulations. D-F were simulated using parameters from LB environments. Asterisks show the parameter values used in the simulations for Figure 1F in LB (black) or SM (red).

Contrary to our expectations, we find that the number of transconjugants after 24h is largely independent of the adsorption rate, and mainly depends on the conjugation rate (Figure 2A, S1A). A high number of transconjugants can be obtained when conjugation rate is increased to values that have been reported in empirical studies [34]. Similarly, the number of newly formed lysogens is primarily determined by the adsorption rate, with optimal conditions for lysogen formation at intermediate rates around 10^{-6} to 10^{-7} (Figure 2B, S1B), which is at the lower end of empirically measured values [24]. However, for the emergence of double-carriers, both conjugation as well as adsorption rates are limiting, producing a narrower window for high cell numbers (Figure 2C, S1A, S1B). Again, optimal conditions can be found at intermediate adsorption rates (Figure 2C), as high adsorption rates will lead to increased killing of plasmid-carriers and recipients by induced phages early on in the infection - which decreases both, plasmid and phage spread. The best fit for the adsorption parameter in the SM environment already coincides with the optimal lysogen formation

489 rate, but plasmid and double-carrier numbers could be increased through a higher conjugation rate
490 (Figure 2A,2C).

491 When we varied the probability to make a decision for lysogeny, we also observed the highest
492 numbers of newly formed lysogens and double-carriers at intermediate values (Figure S2). That is,
493 because variations in lysogenization probability determine the number of productively infecting
494 phages and hence of free phages, which affect the magnitude of phage infections in a similar manner
495 as the adsorption rate. The number of transconjugants is again independent of changes in
496 lysogenization probability (Figure S2).

497 The formation of transconjugants, lysogens and double-carriers, proved to be only weakly
498 dependent on the induction rate (Figure S3). This parameter mainly determines the timing of the
499 phage infection onset but has little influence on final cell numbers after 24h (as long as the epidemic
500 can still take off before bacteria reach stationary phase).

501 Despite the dependence of phage and plasmid infection parameters on bacterial growth phase
502 (i.e., exponential versus stationary growth), variations in bacterial growth rate have little influence on
503 final numbers of the individual subpopulations (Figure 2D-F). A higher starting bacterial density (3-
504 4 orders of magnitude) however, can increase the number of transconjugants and double-carriers at
505 24h by an order of magnitude (Figure 2D, 2F). This indicates that even for the same plasmid-phage
506 combination the number of transconjugants can be different depending on the population densities at
507 the onset of infection – as would also be the case without the presence of phages.

508

509 *One-donor-species experiments show reversed population dynamics*

510 In order to test our model predictions, we performed an experiment with a higher starting bacterial
511 density, which should increase the number of transconjugants and double-carriers. This trend was
512 predicted to be even stronger when we considered only one donor that carried both, the phage and the
513 plasmid (Figure 3A, S4, S7). By doing so, we gave plasmids an additional advantage as plasmid
514 donors could not be killed by released phages.

515 Surprisingly, while transconjugants and double-carriers were indeed appearing at substantially
516 higher numbers in all of the experiments with a single donor, the model neither predicted the
517 drastically lower numbers of lysogens observed in the experiments (meaning that newly formed
518 lysogens were quickly transformed into double-carriers), nor the significant increase in
519 transconjugants above values observed in the mono-culture experiment (Welch's two sample *t*-test:
520 $t_{7.92}$=-4.88, p=0.001; Figure 1, 3, S7). Even the increased adsorption rate in the SM environment did
521 not alleviate the decrease in lysogen numbers. The model fit could only be improved by decreasing
522 phage adsorption, increasing plasmid conjugation and assuming preferential infection of recipients
523 already carrying either the prophage or the plasmid (Figure S7, S8). Using this set of parameters
524 would also increase the absolute number of transconjugants and double-carriers substantially in the
525 2-donor simulations (Figure S9), indicating that the simulations are not able to capture all biologically
526 relevant interactions in this system.
527

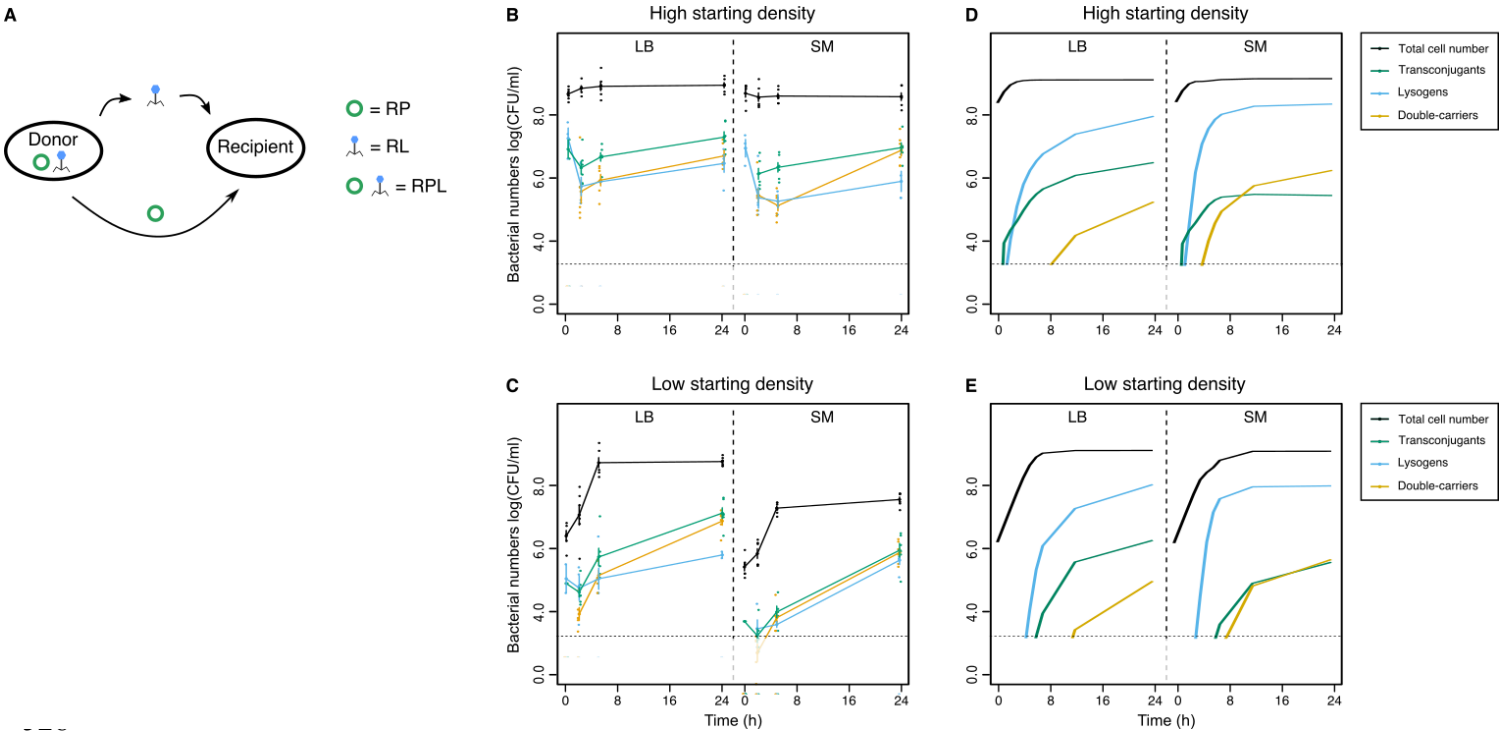

529 **Figure 3 One-donor experiment**. (A) A single donor carrying the plasmid and the phage was mixed with recipient cells.
530 Transconjugants are recipients, which acquired the plasmid (green), lysogens are recipients, which acquired the prophage (blue), and
531 double-carriers are recipients, which acquired the plasmid and the phage (yellow). (B, C) Total population size (black) as well as newly
532 formed lysogens (blue), transconjugants (green), and double-carriers (yellow) measured as colony forming units log10(CFU/ml) over
533 time in LB (left panel) or SM (right panel) starting with high (B) or low (C) bacterial densities. (D, E) Predictions of model simulations
534 for phage and plasmid transfer with a single donor in LB (left panel) or SM (right panel) starting with high (B) or low (C) bacterial
535 densities (colours as indicated for experiments).

Another unexpected observation in this one-donor experiment was the rapid emergence of transconjugants at the first measurement point (Figure 3B, 3C), which did not allow us to estimate the initial rate of increase in those experiments. This might be caused by induction of lysogens continuously killing a small part of the plasmid donor population, meaning that overnight cultures might undergo more turnover [35] and that a larger fraction of the population might still be capable of conjugation [16].

Discussion

Here, we present the first investigation into the dynamics of plasmid spread in the presence of temperate phages. While we observe the intuitive effect of all phages – killing of bacterial cells - we also show the complexity in understanding the magnitude and impact of this death factor in different environments when considering temperate phages. Our results open up new avenues of exploration and set up expectations for plasmid evolution in nature.

Already the comparison between plasmid and phage transfer in mono-culture (Figure 1B) revealed interesting differences in their transfer dynamics: while lysogenization occurred rapidly after mixing with recipient cells, plasmid conjugation showed a lag of several hours. This is surprising, given that for phage infection and subsequent lysogenization to occur, prophages first have to be induced (which happens at a low spontaneous rate) and need to reach a high enough phage-to-bacteria ratio for lysogenization to take place at a significant frequency [7, 8]. In agreement with our data however, it has been shown before that conjugation frequency for some plasmids increases only slowly over the exponential growth phase and peaks at the transition to stationary phase [16]. Another, mutually non-exclusive, explanation could be that recipients pay a plasmid acquisition cost (in addition to the plasmid metabolic burden), which slows down initial growth and spread of transconjugants [36]. Even though transconjugants increased at a significantly slower rate than lysogens (Figure 1B), they increased for longer than the lysogen subpopulation, even after the total bacterial population reached stationary phase. These non-trivial and unequal transfer dependencies on host cell physiology were crucial in model reproduction of empirical observations. While these dependencies have been studied for each system in isolation [16, 20], the outcome of their respective transfer dynamics in environments with plasmids and prophages are hard to predict and will require further experiments to understand the influence of host physiology on concomitant infection dynamics of phages and plasmids.

Our experimental work showed that spontaneous induction of prophages in co-cultures with phage-susceptible plasmid donor and recipient cells can limit plasmid transfer: while the initial rate

569 of increase was only significantly lower in one environment (SM), the total number of transconjugants
570 was significantly reduced in both environments (Figure 1D). Such phage-mediated negative impacts
571 on plasmid spread and existence have also been reported for lytic phages [6]. The situation is less
572 obvious when considering temperate phages, whose potential for killing cells depends not only on
573 bacterial numbers, but also on phage density, often producing only a relatively short burst of (notable)
574 lytic activity [3, 18]. Additionally, plasmids in double-carrier cells are protected from further
575 infection of (related) phages by the resident prophage. Hence, the presence of prophages during
576 conjugation assays could distort the measurement of conjugation rates, potentially showing
577 environmental or growth rate dependencies caused by other factors than plasmid transfer.

578 Overall, transconjugant dynamics in the presence of lysogens can be approximated by interpreting
579 phages as an additional (though strongly environment-dependent) death rate for non-lysogen cells
580 (Figure S10). As prophages are pervasive in natural isolates [3], these findings are highly relevant for
581 understanding the spread of mobile genetic elements, like plasmids, in natural environments. Our
582 model predicted for example that plasmids should evolve high conjugation rates in prophage-rich
583 environments in order to overcome the inhibition through phage killing (Figure 2, S1). As high
584 conjugation rates lead to a high number of plasmid-carriers and double-carriers even at low phage
585 donor and recipient numbers, the ability to overcome the 'phage death rate' is largely independent of
586 phage infection parameters, and hence valid for any particular prophage type. Furthermore, the ability
587 of some plasmid types to conjugate at normal or even higher rates during stationary phase [37] could
588 be an attempt at 'catching up' while most temperate (and many lytic) phages are unable to propagate.

589 Phage killing of cells, on which the phages, but also the plasmids, rely for survival, introduces a
590 feedback into the system, which results in a complex dependence of infection dynamics on
591 environmental conditions. We found that under conditions advantageous for plasmid-carriers (a
592 single plasmid-phage donor and lower initial host availability for phage replication) lysogen transfer
593 was strongly reduced, far beyond what our empirically parametrized model predicted - even when
594 adjusting phage and plasmid transfer rates in a reasonable range around the rates fitted from the mono-

595 culture and two-donor experiments. The model was also not able to reproduce the abundance of
596 double-carriers, which was either overestimated in the two-donor experiment or underestimated in
597 the one-donor experiment. This indicates that the biological processes involved in the formation of
598 double-carriers are more complex then assumed. Those processes could for instance include
599 interactions between phage and plasmid defence and anti-defence mechanisms, such as restriction-
600 modification (RM) and anti-restriction systems, which can be encoded on plasmids [38], and phages
601 [39]. The Rp4 plasmid, as well as the lambda prophage, used in this study both encode anti-restriction
602 systems, which have been shown to be active against the RM-system EcoK in *E. coli* [39, 40].
603 However, our lab strain MG1665 (K12) does, to our knowledge (https://international.neb.com/tools-
604 and-resources/usage-guidelines/restriction-of-foreign-dna-by-e-coli-k-12), not carry EcoKI or other
605 type II restriction systems, which would render the above mentioned anti-restriction systems inactive.
606 Hence, our model analysis suggests more general, yet unknown, interactions between phages and
607 plasmids during concomitant or sequential infection.

608 Besides their role in killing susceptible bacteria, temperate phages can also transfer genes
609 horizontally via a plethora of mechanisms, including specialized and generalized transduction
610 (packaging of non-phage genes) or expression of genes that are potentially beneficial for the host in
611 the prophage state (lysogenic conversion) [41]. In our two-donor experiment, conjugation rate seemed
612 to be the limiting factor for the number of transconjugants and double-carriers. Hence, we expect that
613 in environments or plasmid types where conjugation rates are low, prophages would be more efficient
614 resistance or virulence gene spreaders (Figure 2). Similarly, in environments with prophage types
615 characterized by low adsorption rates we expect plasmids to be the dominant spreader of resistance
616 or virulence genes. If conjugation and adsorption rate both are relatively high, double carriers will be
617 abundant and horizontal gene transfer should be efficient via both, plasmids and temperate phages.
618 As accessory genes, capable of increasing bacterial fitness in a specific environment, need to be
619 transferred by the preferred mode in that environment, interactions between prophages and plasmids
620 could be instrumental in determining the location of horizontally transferred genes.

In summary, we find that the presence of active prophages in the environment limits plasmid transfer by introducing an additional death rate, the magnitude of which however is determined by the specific population dynamics and non-trivial to predict for different environmental conditions. Notably, either prophages or plasmids can increase their own transfer largely independently of the specific plasmid-prophage pair.

626 **References**

627 [1] Benz, F., Huisman, J. S., Bakkeren, E., Herter, J. A., Stadler, T., Ackermann, M., Diard, M.,
628 Egli, A., Hall, A. R., Hardt, W. D., et al. 2020 Plasmid- and strain-specific factors drive variation in
629 ESBL-plasmid spread in vitro and in vivo. *Isme J*. (DOI:10.1038/s41396-020-00819-4).
630 [2] Silver, S. & Misra, T. K. 1988 Plasmid-Mediated Heavy-Metal Resistances. *Annual Review of*
631 *Microbiology* **42**, 717-743. (DOI:DOI 10.1146/annurev.mi.42.100188.003441).
632 [3] Howard-Varona, C., Hargreaves, K. R., Abedon, S. T. & Sullivan, M. B. 2017 Lysogeny in
633 nature: mechanisms, impact and ecology of temperate phages. *Isme J* **11**, 1511-1520.
634 (DOI:10.1038/ismej.2017.16).
635 [4] Proctor, L. M. & Fuhrman, J. A. 1990 Viral Mortality of Marine-Bacteria and Cyanobacteria.
636 *Nature* **343**, 60-62. (DOI:Doi 10.1038/343060a0).
637 [5] Bouvier, T. & del Giorgio, P. A. 2007 Key role of selective viral-induced mortality in
638 determining marine bacterial community composition. *Environ Microbiol* **9**, 287-297.
639 (DOI:10.1111/j.1462-2920.2006.01137.x).
640 [6] Harrison, E., Wood, A. J., Dytham, C., Pitchford, J. W., Truman, J., Spiers, A., Paterson, S. &
641 Brockhurst, M. A. 2015 Bacteriophages limit the existence conditions for conjugative plasmids.
642 *Mbio* **6**, e00586. (DOI:10.1128/mBio.00586-15).
643 [7] Kourilsky, P. 1973 Lysogenization by bacteriophage lambda. I. Multiple infection and the
644 lysogenic response. *Mol Gen Genet* **122**, 183-195.
645 [8] Kobiler, O., Rokney, A., Friedman, N., Court, D. L., Stavans, J. & Oppenheim, A. B. 2005
646 Quantitative kinetic analysis of the bacteriophage lambda genetic network. *Proc Natl Acad Sci U S*
647 *A* **102**, 4470-4475. (DOI:10.1073/pnas.0500670102).
648 [9] Johnson, A. D., Poteete, A. R., Lauer, G., Sauer, R. T., Ackers, G. K. & Ptashne, M. 1981
649 Lambda-Repressor and Cro - Components of an Efficient Molecular Switch. *Nature* **294**, 217-223.
650 (DOI:DOI 10.1038/294217a0).
651 [10] Wendling, C. C., Refardt, D. & Hall, A. R. 2020 Fitness benefits to bacteria of carrying
652 prophages and prophage-encoded antibiotic-resistance genes peak in different environments.
653 *Evolution*. (DOI:10.1111/evo.14153).
654 [11] Burns, N., James, C. E. & Harrison, E. 2015 Polylysogeny magnifies competitiveness of a
655 bacterial pathogen in vivo. *Evol Appl* **8**, 346-351. (DOI:10.1111/eva.12243).
656 [12] Casjens, S. 2003 Prophages and bacterial genomics: what have we learned so far? *Mol*
657 *Microbiol* **49**, 277-300. (DOI:Doi 10.1046/J.1365-2958.2003.03580.X).
658 [13] Gullberg, E., Albrecht, L. M., Karlsson, C., Sandegren, L. & Andersson, D. I. 2014 Selection
659 of a multidrug resistance plasmid by sublethal levels of antibiotics and heavy metals. *Mbio* **5**,
660 e01918-01914. (DOI:10.1128/mBio.01918-14).
661 [14] Lenski, R. E., Rose, M. R., Simpson, S. C. & Tadler, S. C. 1991 Long-Term Experimental
662 Evolution in Escherichia-Coli .1. Adaptation and Divergence during 2,000 Generations. *Am Nat*
663 **138**, 1315-1341. (DOI:Doi 10.1086/285289).
664 [15] Levin, B. R., Stewart, F. M. & Rice, V. A. 1979 The kinetics of conjugative plasmid
665 transmission: fit of a simple mass action model. *Plasmid* **2**, 247-260. (DOI:10.1016/0147-
666 619x(79)90043-x).
667 [16] Headd, B. & Bradford, S. A. 2020 The Conjugation Window in an Escherichia coli K-12 Strain
668 with an IncFII Plasmid. *Appl Environ Microbiol* **86**. (DOI:10.1128/AEM.00948-20).
669 [17] Kourilsky, P. 1975 Lysogenization by bacteriophage lambda. *Biochimie* **56**, 1511-1516.
670 [18] Pleska, M., Lang, M., Refardt, D., Levin, B. R. & Guet, C. C. 2018 Phage-host population
671 dynamics promotes prophage acquisition in bacteria with innate immunity. *Nat Ecol Evol* **2**, 359-
672 366. (DOI:10.1038/s41559-017-0424-z).
673 [19] Rodriguez-Gonzalez, R. A., Leung, C. Y., Chan, B. K., Turner, P. E. & Weitz, J. S. 2020
674 Quantitative Models of Phage-Antibiotic Combination Therapy. *mSystems* **5**.
675 (DOI:10.1128/mSystems.00756-19).

676 [20] Nabergoj, D., Modic, P. & Podgornik, A. 2018 Effect of bacterial growth rate on bacteriophage
677 population growth rate. *Microbiologyopen* **7**, e00558. (DOI:10.1002/mbo3.558).
678 [21] Weitz, J. S. & Dushoff, J. 2008 Alternative stable states in host–phage dynamics. *Theor Ecol-*
679 *Neth* **1**, 13-19.
680 [22] Bull, J. J., Vegge, C. S., Schmerer, M., Chaudhry, W. N. & Levin, B. R. 2014 Phenotypic
681 resistance and the dynamics of bacterial escape from phage control. *PLoS One* **9**, e94690.
682 (DOI:10.1371/journal.pone.0094690).
683 [23] Huisman, J., Benz, F., Duxbury, S. J. N., de Visser, J. A. G. M., Hall, A. R., Fischer, E. A. J. &
684 Bonhoeffer, S. 2020 Estimating the rate of plasmid transfer in liquid mating cultures. *biorxive*.
685 (DOI:https://doi.org/10.1101/2020.03.09.980862).
686 [24] Gill, J. J. 2009 Modeling of bacteriophage therapy. *Bacteriophage Ecol.*, 439-464.
687 (DOI:doi:10.1017/cbo9780511541483.020).
688 [25] Storms, Z. J., Arsenault, E., Sauvageau, D. & Cooper, D. G. 2010 Bacteriophage adsorption
689 efficiency and its effect on amplification. *Bioprocess Biosyst Eng* **33**, 823-831.
690 (DOI:10.1007/s00449-009-0405-y).
691 [26] Sheppard, R. J., Beddis, A. E. & Barraclough, T. G. 2020 The role of hosts, plasmids and
692 environment in determining plasmid transfer rates: A meta-analysis. *Plasmid* **108**, 102489.
693 (DOI:10.1016/j.plasmid.2020.102489).
694 [27] Lang, M., Pleška, M. & Guet, C. C. 2020 Population dynamics of decision making in
695 temperate bacteriophages. *bioRxiv* **020.03.18.996918**. (DOI:doi:10.1101/2020.03.18.996918).
696 [28] Refardt, D. & Rainey, P. B. 2010 Tuning a Genetic Switch: Experimental Evolution and
697 Natural Variation of Prophage Induction. *Evolution* **64**, 1086-1097.
698 [29] Cortes, M. G., Krog, J. & Balazsi, G. 2019 Optimality of the spontaneous prophage induction
699 rate. *J Theor Biol* **483**, 110005. (DOI:10.1016/j.jtbi.2019.110005).
700 [30] Berngruber, T. W., Froissart, R., Choisy, M. & Gandon, S. 2013 Evolution of virulence in
701 emerging epidemics. *PLoS Pathog* **9**, e1003209. (DOI:10.1371/journal.ppat.1003209).
702 [31] Moldovan, R., Chapman-McQuiston, E. & Wu, X. L. 2007 On kinetics of phage adsorption.
703 *Biophys J* **93**, 303-315. (DOI:10.1529/biophysj.106.102962).
704 [32] Zatyka, M. & Thomas, C. M. 1998 Control of genes for conjugative transfer of plasmids and
705 other mobile elements. *Fems Microbiol Rev* **21**, 291-319.
706 [33] Shao, Y. & Wang, I. N. 2008 Bacteriophage adsorption rate and optimal lysis time. *Genetics*
707 **180**, 471-482. (DOI:10.1534/genetics.108.090100).
708 [34] Zhang, S., Wang, Y., Song, H., Lu, J., Yuan, Z. & Guo, J. 2019 Copper nanoparticles and
709 copper ions promote horizontal transfer of plasmid-mediated multi-antibiotic resistance genes
710 across bacterial genera. *Environ Int* **129**, 478-487. (DOI:10.1016/j.envint.2019.05.054).
711 [35] Lane, D., Cavaille, J. & Chandler, M. 1994 Induction of the SOS response by IS1 transposase.
712 *J Mol Biol* **242**, 339-350. (DOI:10.1006/jmbi.1994.1585).
713 [36] Prensky, H., Gomez-Simmonds, A., Uhlemann, A.-C. & Lopatkin, A. 2021 Conjugation
714 dynamics depend on both the plasmid acquisition cost and the fitness cost. *Mol Syst Biol* **17**.
715 (DOI:doi.org/10.15252/msb.20209913).
716 [37] Sysoeya, T. A., Kim, Y., Rodriguez, J., Lopatkin, A. J. & You, L. C. 2020 Growth-stage-
717 dependent regulation of conjugation. *Aiche J* **66**. (DOI:ARTN e16848
718 10.1002/aic.16848).
719 [38] Klaenhammer, T. R. 1987 Plasmid-directed mechanisms for bacteriophage defense in lactic
720 streptococci. *FEMS Microbiol Ecol* **46**, 313-325. (DOI:https://doi.org/10.1111/j.1574-
721 6968.1987.tb02468.x).
722 [39] Loenen, W. A. M. & Murray, N. E. 1986 Modification Enhancement by the Restriction
723 Alleviation Protein (Ral) of Bacteriophage-Lambda. *Journal of Molecular Biology* **190**, 11-22.
724 (DOI:Doi 10.1016/0022-2836(86)90071-9).
725 [40] Goryanin, I. I., Kudryavtseva, A. A., Balabanov, V. P., Biryukova, V. S., Manukhov, I. V. &
726 Zavilgelsky, G. B. 2018 Antirestriction activities of KlcA (RP4) and ArdB (R64) proteins. *Fems*
727 *Microbiol Lett* **365**. (DOI:ARTN fny227

728 10.1093/femsle/fny227).
729 [41] Waldor, M. K. & Mekalanos, J. J. 1996 Lysogenic conversion by a filamentous phage
730 encoding cholera toxin. *Science* **272**, 1910-1914.
731